ELSEVIER

Chemical Engineering Journal 137 (2008) 579–586

Chemical Engineering Journal

www.elsevier.com/locate/cej

Study of H-β-zeolite supported Rh catalyst by inverse gas chromatography

Xiali Zhang [a], Linping Qian [b], Peng Xu [a], Heyong He [b], Qiangguo Du [a,*]

[a] *Key Laboratory of Molecular Engineering of Polymers of Ministry of Education, Department of Macromolecular Science, Fudan University, Shanghai 200433, China*

[b] *Shanghai Key Laboratory of Molecular Catalysis and Innovative Materials, Department of Chemistry, Fudan University, Shanghai 200433, China*

Received 14 January 2007; received in revised form 10 May 2007; accepted 16 May 2007

Abstract

Catalysts containing rhodium (Rh) were prepared by the wet impregnation method using H-β-zeolite as support. Retention time of three *n*-alkanes (C_5–C_7), cyclohexane, benzene, trichloroethylene and tetrachloroethylene on the Rh/H-β-zeolite catalysts (0.5–2.0 wt% of Rh) and H-β-zeolite were measured by inverse gas chromatography (IGC) in the 473.2–513.2 K temperature range. Standard free energy of adsorption, dispersive component of surface free energy of adsorbent and specific interaction parameters between polar probes and catalysts were evaluated. The results indicate that the adsorption characteristics of H-β-zeolite can be modified by rhodium. Surface area, enthalpy of adsorption and dispersive component of surface free energy decrease after the impregnation of rhodium. Besides, it was found that rhodium dispersed in the framework of H-β-zeolite had special adsorption for benzene which may be useful for making catalysts for certain reactions involving benzene in the future.

Keywords: Inverse gas chromatography; Rhodium; H-β-zeolite; Adsorption; Catalyst

1. Introduction

Up to now, rhodium-containing catalysts play a very important role in industrial processes [1–3]. One of the important applications is to clean up pollutants. For example, rhodium is used in the manufacture of automobile catalytic converts [4]. It is an active catalyst for oxidations of ammonia and carbon monoxide and the elimination of nitric oxide [5,6]. Rh/Al_2O_3 and Rh/H-BEA were successfully used for synthesis of gas from CO_2 reforming of methane [7–9]. Beta zeolite was reported to be a promising catalyst in most literatures, because it possesses relatively high density of Brønsted acid sites and favorable pore structure [10–12]. Zeolite is also a suitable support for noble metals or metal oxides due to their open structure and ion exchange capacities in heterogeneous catalysts. There have been several studies on the adsorption properties of zeolite and metal loaded zeolite [13], but to our knowledge there are no detailed studies on the adsorption parameters of H-β-zeolite supported rhodium catalysts.

Gas–solid chromatography has been used for many years to study adsorption and catalytic reactions with some advantages with respect to static methods [14]. In contrast to conventional gas chromatography, inverse gas chromatography (IGC) has the stationary phase of the system as the object of interest while the vapor of materials of known properties as probes. IGC measurement can provide information on thermodynamic parameters, surface energy, reaction kinetics, and textural parameters such as surface area and porosity. It is a fast and easily controlled method. IGC has been widely utilized to study synthetic and biological polymers [15], copolymers [16], polymer blends [17], adsorbents [18], foods [19], carbon blacks [20], fibers [21], clays [22], and catalysts [23–31]. In recent years, Diaz et al. [14,25–29,31] reported numerous studies on the surface of catalysts using inverse gas chromatography. Probably the main drawback of the method is that IGC only provides physicochemical properties of the stationary statistically independent of time. It ignores the heterogeneity

* Corresponding author. Tel.: +86 21 6564 3891; fax: +86 21 6564 0293.
E-mail address: qgdu@fudan.edu.cn (Q. Du).

1385-8947/$ – see front matter © 2007 Elsevier B.V. All rights reserved.
doi:10.1016/j.cej.2007.05.020

of the adsorbing solid surface [32]. Time-resolved gas chromatography was invented to overcome these difficulties. The results of reversed-flow gas chromatography (RF-GC) do not need extrapolation to infinite dilution and zero carrier gas flow-rate to approximate true physicochemical parameters [33]. RF-GC permitted a direct determination of catalytic reaction rate constants, adsorption–adsorption rate constants, gas and surface diffusion coefficients, adsorption isotherm parameters, etc. [32–35]

In the present work, the surface properties of H-β-zeolite and Rh/H-β-zeolite, the heat of adsorption, the free energy of adsorption, the surface free energy, as well as their specific and dispersive components, were investigated by IGC. The chromatographic data should provide information on the interaction between the sorbed molecules and the catalyst or the support, and lead to insight on the catalytic behavior of rhodium.

2. Experimental

2.1. Catalyst preparation

Five grams of H-β-zeolite (n(Si)/n(Al) = 12.5, Nankai University) was impregnated with appropriate volume of $RhCl_3 \cdot 3H_2O$ (98%, Aldrich) solution (0.1 mol L^{-1}) to prepare the catalyst containing Rh by the incipient wet impregnation method [36]. After drying under an infrared lamp, the catalysts were calcined at 573 K in air with a flow rate of 100 cm^3 min^{-1} for 30 min and then reduced at 773 K in H_2 with a flow rate of 20 cm^3 min^{-1} for 60 min.

2.2. Surface area measurement

The surface area of adsorbents was measured using N_2 physisorption at 77 K. Prior to measurement, samples were transferred to the glass adsorption tube and were degassed at 383 K under ultrapure nitrogen flow for 2.0 h. The nitrogen adsorption–desorption isotherms were acquired on the Micromeritics Tristar 3000 apparatus. The pore volume was calculated from the so-called t-plot. The surface area was calculated from Langmuir desorption isotherms.

2.3. Transmission electron microscopy (TEM)

The structure of the four samples was detected with transmission electron microscopy (TEM). The investigations were performed on a JEOL JEM-2010 microscope. The samples for TEM were prepared by adding 1–2 drops of solution of the catalyst in ethanol onto lacey carbon copper grids.

2.4. The X-ray powder diffraction (XRD)

The crystalline structure of catalysts was determined by X-ray powder diffraction (XRD). The XRD patterns of samples were recorded on an X′ Pert PRO (PANalytical) diffractometer at room temperature with Cu Kα radiation. XRD diagrams were obtained in the range of $2\theta = 10$–50° by step scanning with a step size of 0.017°.

2.5. IGC apparatus and procedure

The chromatographic experiments were performed with a GC112A gas chromatography equipped with a flame ionization detector. Retention times were recorded on a workstation N2000.

High purity nitrogen was used as the carrier gas with a flow rate of about 28 mL min^{-1}. The flow rate of the carrier gas was measured with a soap bubble flowmeter and was corrected using James–Martin factor for pressure drop and temperature change in the column.

The adsorbates (probes) used were *n*-pentane, *n*-hexane, *n*-heptane, cyclohexane, trichloroethylene, tetrachloroethylene, and benzene. The probes of analytical reagent grade were purchased from Shanghai Chemical Reagents Company and used without further purification.

Samples were compacted into wafers using a press at 20 tonnes pressure. Then the pressed wafers were crumbled and sieved to obtain the powdery aggregates of 60–80 mesh in size. A stainless steel column (30 cm long, 2 mm i.d.) cleaned with methanol and acetone was used in this work. The column was filled with 0.2 g (ca.) of the resulting powder with the aid of vacuum and mechanical vibration. The two ends of the column were plugged with silane-treated glass wool. The column was then stabilized on the GC system at 513.2 K overnight under a nitrogen flow of 28 mL min^{-1}. In order to avoid detector contamination, the outlet of the column was not connected to the detector during this treatment period.

Measurements were carried out in the temperature range from 473.2 to 513.2 K. In order to meet the requirement of adsorption at infinite dilution, corresponding to zero coverage and GC linearity, the probes were introduced into the column using a 1 μL syringe and the injected vapor volumes were lower than 0.1 μL. Therefore, any solute–solute interaction can be neglected and the retention on the solid surface is only governed by solid–probe interactions. For each measurement, at least three repeated injections were made to obtain reproducible results. Methane was used as a marker for the retention-time correction, which was used to ensure the absence of dead volume when a new column was placed in the chromatography. The net retention volume, V_N, can be calculated from the measured retention time t_R.

3. Calculations

3.1. Standard free energy of adsorption: specific and dispersive components

At infinite dilution, the standard free energy to transfer 1 mol of adsorbate from the gas phase to the surface at standard state, defined as the variation in the standard free energy of adsorption,

ΔG_{ads} (J mol^{-1}), is given by the following equation:

$$\Delta G_{ads} = -RT_C \ln \frac{K_s p_{s,g}}{\pi_s} \quad (1)$$

where K_s is the surface partition coefficient, $p_{s,g}$ the adsorbate vapor pressure in the gaseous standard state and π_s is the vapor pressure at equilibrium with the standard adsorption state (the De Boer standard state).

For surface adsorption,

$$V_N = K_s A \quad (2)$$

$$A = mS \quad (3)$$

Then ΔG_{ads} can be expressed as

$$\Delta G_{ads} = -RT_C \ln \frac{V_N p_{s,g}}{\pi_s m S} \quad (4)$$

where R is the gas constant, A the specific surface area, m the mass of adsorbent in the column and S is the specific surface area of adsorbent. The standard reference states were taken as $p_{s,g} = 101$ kN m^{-2} (1 atm) and $\pi_s = 0.338$ mN m^{-1}, the value of the latter was proposed by De Boer [37].

For a given adsorbate, the surface free energy, ΔG_{ads} (J mol^{-1}), is the sum of energies of adsorption attributed to dispersive, ΔG^D_{ads}, and specific, ΔG^S_{ads}, interactions.

For n-alkanes $\Delta G_{ads} = \Delta G^D_{ads}$, the increment of adsorption energy corresponding to methylene group, ΔG_{CH_2}, can be calculated from

$$\Delta G_{CH_2} = -RT_C \ln \frac{V_{N(n)}}{V_{N(n+1)}} \quad (5)$$

where $V_{N(n)}$ and $V_{N(n+1)}$ are the retention volume of n-alkanes with (n) and $(n+1)$ carbon atoms, respectively.

The surface free energy of the adsorbent, γ_S, may be split into dispersion, γ^D_S, and specific, γ^S_S, contributions:

$$\gamma_S = \gamma^D_S + \gamma^S_S \quad (6)$$

The dispersive component of the surface energy (γ^D_S), intrinsic and unspecific for all molecules, is due to London forces. It is given by the following equation:

$$\gamma^D_S = \frac{1}{4} \frac{\Delta G^2_{CH_2}}{\gamma_{CH_2} N^2 a^2_{CH_2}} \quad (7)$$

where N is the Avogadro's number, a_{CH_2} the cross sectional area occupied by a $-CH_2-$ group (0.06 nm^2), and γ_{CH_2} (mJ m^{-2}) is the surface tension of a surface consisting of CH_2 groups, which has the following expression:

$$\gamma_{CH_2} = 35.6 + 0.058(20 - T_C) \quad (8)$$

The specific component of the surface free energy is closely related to the parameter of specific interaction of polar solutes I^{SP}. This parameter involves the surface properties in terms of potential and acid–base interactions and may be determined from the difference of free energy of adsorption, $\Delta(\Delta G)$, between a polar solute and the real or hypothetical n-alkane with the same cross-section surface area [24] or boiling point, T_b [38], as shown in the following equation:

$$I^{SP} = \frac{\Delta(\Delta G)}{Na_p} \quad (9)$$

where a_p is the cross sectional area of the polar probe. In this work, a_p is calculated from the liquid density, ρ, and the molar weight of the probe, M, assuming molecules of spherical shape in a hexagonal close-packed configuration [31,38].

$$a_p = 1.09 \times 10^{14} \left(\frac{M}{\rho N} \right)^{2/3} \quad (10)$$

Although this treatment is empirical, it enables the comparison of the specific interaction between the catalyst and the probe molecule by means of a unified scale.

3.2. Enthalpy of adsorption

The heat of adsorption ΔH_{ads} can be calculated from Gibbs–Helmotz equation

$$\frac{\partial(\Delta G_{ads}/T_C)}{\partial T_C} = -\frac{\Delta H_{ads}}{T^2_C} = -R \frac{\mathrm{d} \ln V_N}{\mathrm{d} T_C} \quad (11)$$

thus

$$\Delta H_{ads} = -R \frac{\partial(\ln V_N)}{\partial(1/T_C)} \quad (12)$$

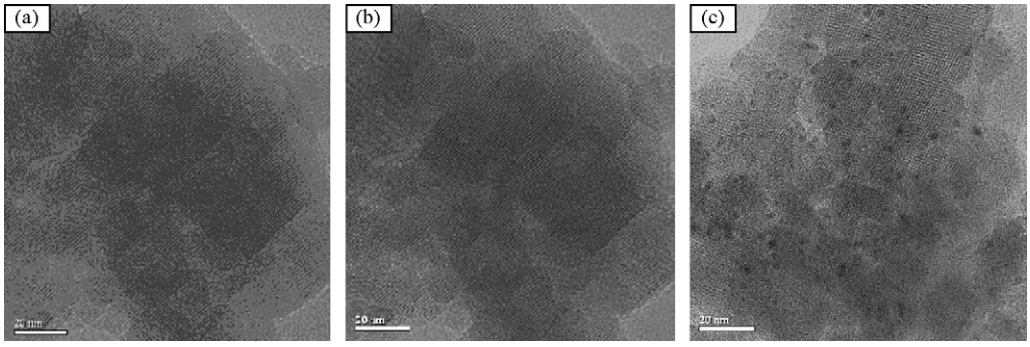

Fig. 1. TEM images of 0.5% Rh/H-β-zeolite (a), 1.0% Rh/H-β-zeolite (b) and 2.0% Rh/H-β-zeolite (c).

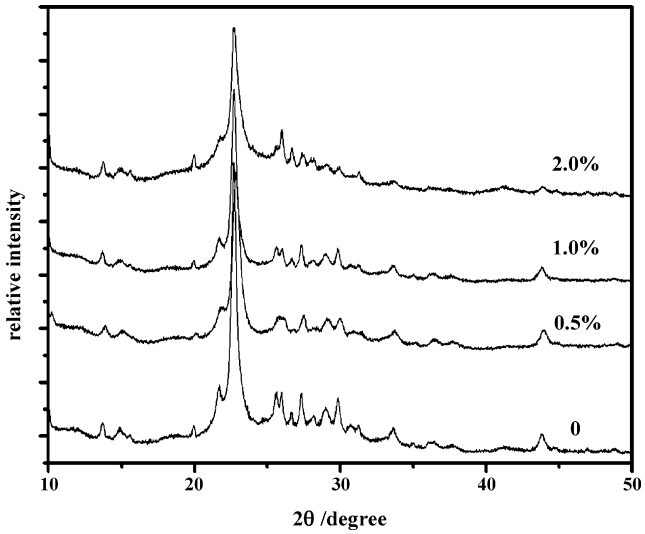

Fig. 2. XRD patterns of H-β-zeolite and Rh/H-β-zeolite.

4. Results and discussion

4.1. Catalysts characterization

Fig. 1 shows the transmission electron microscopy (TEM) images of H-β-zeolite and the Rh loaded H-β-zeolite. It is notable that for the H-β-zeolite loaded with 2.0% rhodium, there are uniform nanoparticles with about 2 nm average diameter and these nanoparticles distribute evenly in the zeolite framework. The nanoparticles are different from zeolite in nature and it is suggested that they are rhodium metal particles. Except for the H-β-zeolite loaded with 2.0% rhodium, there is no visible presence of particles under TEM and it is suggested that the rhodium metal is dispersed uniformly in the zeolite framework in much smaller size. From the pictures it also can be observed that the impregnation of metal did not significantly affect the shape of the parent zeolite.

The X-ray diffraction patterns of H-β-zeolite-supported rhodium catalysts are shown in Fig. 2 alongside the pattern of pure H-β-zeolite. The high-intensity line ($2\theta = 22.7^\circ$) is attributed to zeolite beta. It can be seen from the figure that all samples exhibit the typical diffractograms of zeolite beta framework. The intensities of the zeolite lines decrease slightly with the addition of Rh, indicating that the crystallinity of the zeolite is decreasing when increasing Rh loading.

Table 1
Specific surface area of catalysts

Sample	$S_{Langmuir}$ ($m^2\ g^{-1}$)	V_{micro} ($cm^3\ g^{-1}$)
H-β-zeolite	675	0.192
0.5% Rh/H-β-zeolite	593	0.169
1.0% Rh/H-β-zeolite	618	0.174
2.0% Rh/H-β-zeolite	553	0.157

The surface area of catalysts obtained is shown in Table 1. From Table 1 it can be observed that the surface area decreases slightly after the impregnation. The result proves that for rhodium loaded zeolite, there are metal particles in the zeolite framework and the metal particles block the micropores thus decrease the microporosity of the zeolites. Considering the inaccuracy of the instruments, the sample of 0.5% Rh is level with the sample of 1.0% Rh in the surface area and pore volume. However, the sample of 2.0% Rh shows much lower surface area and pore volume. This phenomenon can be attributed to their difference in the particle size. For the samples of 0.5% Rh and 1.0% Rh, the Rh particles are not large enough to block the channels of the zeolite. When Rh-loading reaches around 2.0%, the nanoparticles are large enough to be visible under TEM and block the micropores greatly, thus decrease the surface area and the pore volume obviously.

4.2. Inverse gas chromatography

4.2.1. Influence of the carrier gas flow rate on measurements

In the measurement of the adsorption characteristics of both Rh/H-β-zeolite and H-β-zeolite, it is important to separate the probe adsorption on the external surface from the probe diffusion within the bulk of the materials. It may be expected that for

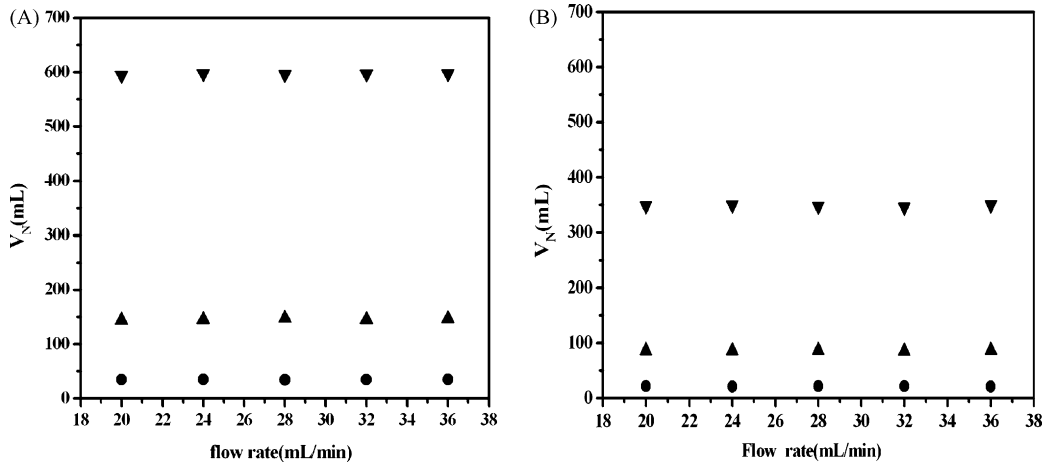

Fig. 3. Influence of carrier gas flow rate on the retention volume at 473.2 K for pentane (●), hexane (▲), heptane(▼) over: (A) 1% Rh/H-β-zeolite and (B) H-β-zeolite.

microporous materials, such as zeolites, this separation is necessary. Mukhopadhyay and Schreiber [39] and Qin and Schreiber [40] have demonstrated that by changing the carrier gas flow rate and thus changing the contact time between adsorbate and adsorbent, it is possible to separate the surface adsorption contribution from the total retention datum.

The retention volume of alkanes is shown in Fig. 3 as a function of the carrier gas flow rate with 1% Rh/H-β-zeolite and H-β-zeolite as stationary phases at 473.2 K. It can be observed that the retention data were independent of the carrier gas flow rate in both instances, which indicates that the measurements are not limited by diffusion effects. According to Fig. 3, a flow rate of 28 mL min^{-1} was chosen for this study.

4.2.2. Standard surface free energy

The standard free energies of adsorption are given in Table 2 calculated from Eq. (4). The decrease of adsorption free energy with the increase of temperature follows the van't Hoff equation. From Table 2 it can be easily observed that the standard free energies of adsorption of benzene to zeolite increase greatly when rhodium is loaded onto zeolite. It also can be observed from the table that the standard free energies of adsorption of H-β-zeolite increased with the Rh loading. It may be caused by the highly dispersive Rh metal particles. The unsaturated Rh surface atoms are more active and contribute to the adsorption of probes. While further increasing Rh loading to 2.0%, the growing size of metal particles started to be visible and blocked the zeolite channels thus stopped the rising of free energies of adsorption.

Dispersive component of surface free energy of adsorbent, γ_S^D, is calculated from Eq. (7) (Fig. 4). The dispersive interaction decreases as the temperature increases, which is attributed to the entropic contribution to the surface free energy. It is observed that most values of the dispersive component of surface free energy of Rh/H-β-zeolite are lower than those of H-β-zeolite

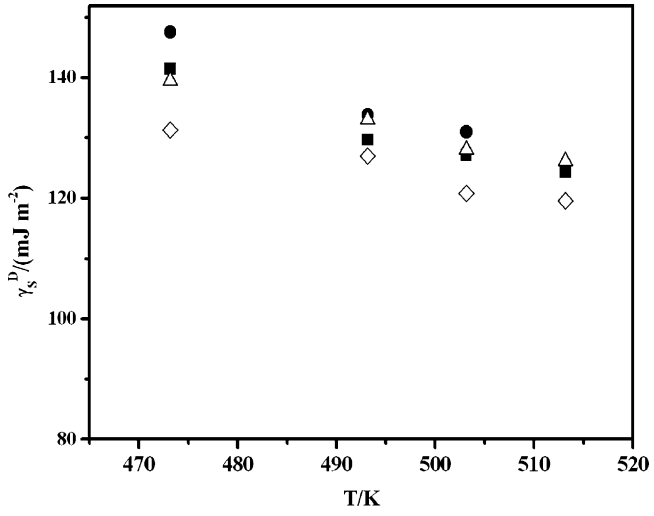

Fig. 4. Dispersive interaction, γ_S^D, of catalysts as a function of temperature (H-β-zeolite (●), 0.5% Rh/H-β-zeolite (△), 1.0% Rh/H-β-zeolite (■) and 2.0% Rh/H-β-zeolite (◊)).

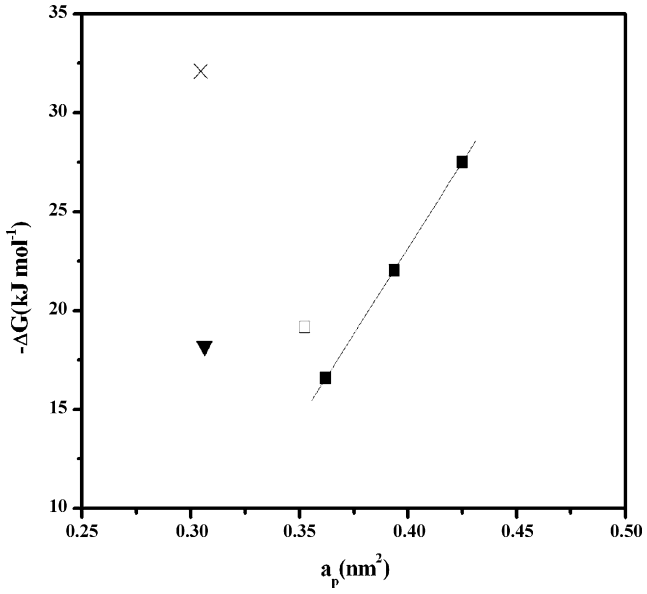

Fig. 5. Specific interaction parameter based on a_p, 1.0% Rh/H-β-zeolite at 493.2 K (*n*-alkanes (■), cyclohexane(□), benzene(×) and trichloroethylene(▼)).

over the temperature range examined. This can be ascribed to the decrease of surface area of zeolite after loaded. From Fig. 4 it is also observed that the γ_S^D values of the surface free energy of Rh/H-β-zeolite vary slightly with the rhodium loading. The γ_S^D values of H-β-zeolite and Rh/H-β-zeolite are a little lower than those of zeolite 13X (154.9 mJ m^{-2} at 200 °C) [14], Al_2O_3 and Pd/Al_2O_3 [28] and NaX and CaA [26] observed by Diaz.

The specific interaction parameter, I^{SP}, can be evaluated from Eq. (9) (Fig. 5). Table 3 shows I^{SP} values of H-β-zeolite, 0.5, 1.0 and 2.0 Rh/H-β-zeolite. It is notable that I^{SP} of H-β-zeolite to benzene increased greatly after rhodium was loaded onto H-β-zeolite.

The interaction between a solid substrate and probes is attributed to secondary bonding caused by both polar and nonpolar (dispersive) Van der Waals forces between adsorbent and adsorbate. Fig. 4 reveales that the amount of Rh loading had very limited effect on the nonpolar forces between zeolite and benzene, indicating that rhodium has special interaction with benzene. The interaction of electrons between aromatic ring and rhodium probably intensifies the physicochemical adsorption of benzene. And, like the standard free energy ΔG_{ads} and dispersive component free energy γ_S^D, it is also observed that the I^{SP} values of Rh/H-β-zeolite increase with the Rh loading. But the I^{SP} values decrease when Rh loading reaches to 2.0%.

4.2.3. Enthalpy of adsorption

Enthalpy of adsorption ΔH_{ads} can be obtained from the slope of the plot of $R \ln V_N$ versus $1/T$ (Fig. 6), based on Eq. (12), and the results are summarized in Table 4. The dependence of adsorption enthalpy on the size of probe molecule on H-β-zeolite and 1.0% Rh/H-β-zeolite is shown in Fig. 6. Linear relationships are observed. High ΔH_{ads} value indicates a strong interaction between catalyst and adsorbate. It is observed that the adsorption enthalpy increases with the number of carbon atoms, due

Table 2
Standard free energy of adsorption, $-\Delta G_{ads}$ (kJ mol^{-1}) for the probes on catalysts

Adsorbent/probe	Temperature (K)			
	473.2	493.2	503.2	513.2
H-β-zeolite				
Pentane	15.59(0.13)	14.17(0.12)	13.53(0.05)	12.73(0.06)
Hexane	21.04(0.05)	19.43(0.05)	18.70(0.04)	17.81(0.02)
Heptane	26.53(0.04)	24.64(0.02)	23.89(0.04)	22.98(0.05)
Cyclohexane	18.75(0.10)	17.32(0.01)	16.61(0.09)	15.91(0.02)
Trichloroethylene	16.59(0.03)	15.15(0.06)	14.42(0.12)	13.87(0.05)
Tetrachloroethylene	18.52(0.05)	17.13(0.04)	16.41(0.06)	15.83(0.03)
Benzene	18.31(0.10)	16.77(0.13)	16.20(0.14)	15.60(0.04)
0.5% Rh/H-β-zeolite				
Pentane	18.28(0.08)	17.09(0.07)	16.36(0.12)	15.88(0.03)
Hexane	23.92(0.09)	22.38(0.01)	21.51(0.05)	21.06(0.03)
Heptane	29.44(0.04)	27.73(0.07)	26.89(0.04)	26.18(0.06)
Cyclohexane	21.04(0.06)	19.49(0.04)	18.78(0.05)	18.14(0.05)
Trichloroethylene	20.02(0.05)	18.76(0.05)	18.17(0.02)	17.75(0.01)
Tetrachloroethylene	22.08(0.09)	20.60(0.04)	19.90(0.05)	19.46(0.03)
Benzene	30.75(0.19)	30.22(0.12)	30.06(0.15)	29.74(0.20)
1.0% Rh/H-β-zeolite				
Pentane	18.40(0.01)	16.89(0.03)	16.42(0.04)	15.69(0.06)
Hexane	23.92(0.04)	22.21(0.09)	21.66(0.16)	20.89(0.12)
Heptane	29.26(0.01)	27.49(0.01)	26.55(0.04)	26.01(0.12)
Cyclohexane	21.41(0.03)	19.72(0.01)	19.05(0.02)	18.42(0.04)
Trichloroethylene	20.07(0.01)	19.91(0.02)	19.10(0.04)	19.02(0.13)
Tetrachloroethylene	21.78(0.08)	21.33(0.04)	20.64(0.03)	20.03(0.07)
Benzene	32.35(0.14)	32.44(0.12)	32.09(0.10)	31.92(0.19)
2.0% Rh/H-β-zeolite				
Pentane	16.63(0.09)	15.34(0.15)	14.63(0.05)	13.91(0.06)
Hexane	21.99(0.12)	20.65(0.03)	19.90(0.14)	19.23(0.19)
Heptane	27.16(0.04)	25.69(0.20)	24.68(0.04)	23.97(0.02)
Cyclohexane	19.18(0.12)	18.18(0.08)	17.45(0.03)	17.28(0.08)
Trichloroethylene	18.76(0.03)	17.46(0.16)	16.95(0.08)	16.21(0.07)
Tetrachloroethylene	20.33(0.04)	19.16(0.03)	18.55(0.08)	17.82(0.04)
Benzene	29.88(0.40)	27.89(0.33)	27.06(0.29)	26.07(0.31)

Standard deviations are given in parentheses.

to the increasing boiling point of the *n*-alkanes and the stronger interaction between the probe and the adsorbent surface. It is also observed that the adsorption enthalpies of *n*-alkanes on H-β-zeolite are higher than those on Rh/H-β-zeolite. It may be attributed to the Lewis acid sites in H-β-zeolite that are active for the adsorption of hydrocarbons. Similar observations were reported in the literature [28]. In addition, it can be seen that, for these compounds, the values of ΔH_{ads} are higher than their corresponding heat of liquefaction (Table 4). This implies that the measured enthalpies of adsorption are not only from the

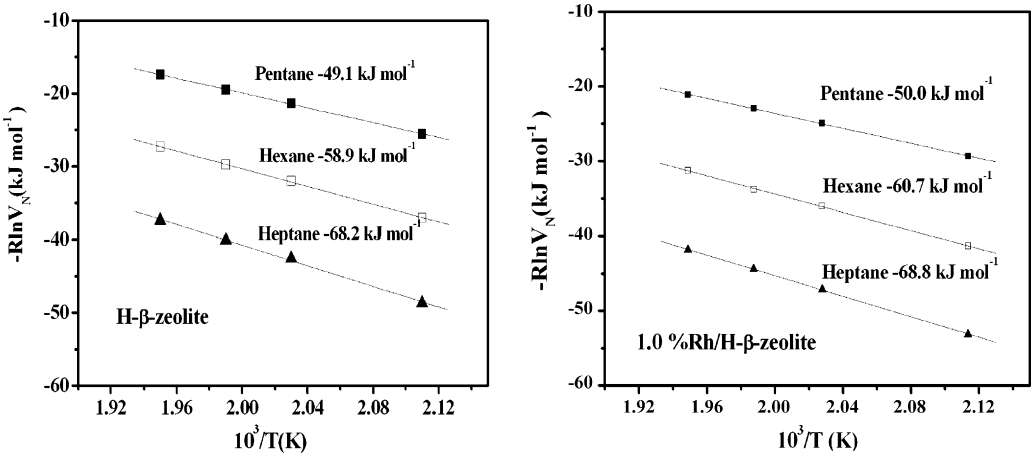

Fig. 6. Adsorption enthalpies (ΔH_{ads}) of *n*-alkanes on catalysts.

Table 3
I^{SP} (mJ m^{-2}) values determined for catalysts under study

Adsorbent/probe	Temperature (K)			
	473.2	493.2	503.2	513.2
H-β-zeolite				
Cyclohexane	22.9(0.5)	22.5(0.1)	22.1(0.4)	22.6(0.1)
Trichloroethylene	58.1(0.2)	55.7(0.3)	54.7(0.7)	55.6(0.3)
Tetrachloroethylene	44.2(0.3)	43.0(0.2)	42.4(0.3)	43.3(0.1)
Benzene	69.5(0.5)	66.4(0.7)	66.3(0.8)	66.9(0.4)
0.5% Rh/H-β-zeolite				
Cyclohexane	21.1(0.3)	19.1(0.2)	19.3(0.2)	18.1(0.3)
Trichloroethylene	63.1(0.3)	60.3(0.3)	60.7(0.1)	59.7(0.1)
Tetrachloroethylene	43.4(0.4)	40.9(0.2)	41.0(0.3)	40.4(0.2)
Benzene	123.6(1.0)	125.7(0.7)	127.5(0.8)	127.0(1.1)
1.0% Rh/H-β-zeolite				
Cyclohexane	22.0(0.2)	21.1(0.1)	19.5(0.1)	20.4(0.2)
Trichloroethylene	66.6(0.1)	67.4(0.1)	63.0(0.2)	67.7(0.7)
Tetrachloroethylene	45.5(0.4)	45.4(0.2)	43.0(0.1)	44.2(0.4)
Benzene	135.6(0.8)	137.7(0.7)	135.8(0.6)	140.0(1.0)
2.0% Rh/H-β-zeolite				
Cyclohexane	19.6(0.5)	20.7(0.4)	20.3(0.2)	22.8(0.4)
Trichloroethylene	62.1(0.2)	61.1(0.9)	60.5(0.4)	60.4(0.4)
Tetrachloroethylene	41.4(0.2)	41.6(0.2)	41.2(0.4)	41.1(0.2)
Benzene	124.7(2.2)	119.9(1.8)	117.6(2.6)	116.1(1.7)

Standard deviations are given in parentheses.

Table 4
Adsorption enthalpies $-\Delta H_{ads}$ (kJ mol^{-1}) and solute liquefaction heats for the compounds studied over the different adsorbents

Probe	H-β-zeolite	0.5% Rh/H-β-zeolite	1% Rh/H-β-zeolite	2% Rh/H-β-zeolite	$-\Delta H_{liq}$ (kJ mol^{-1})
Pentane	49.1(0.999)	47.2(0.998)	50.0(0.999)	48.7(0.999)	24.3
Hexane	58.9(0.999)	58.7(0.997)	60.7(0.999)	54.8(0.999)	27.2
Heptane	68.2(0.999)	68.4(0.999)	68.8(0.999)	65.3(0.998)	31.7
Cyclohexane	52.4(0.999)	55.6(0.999)	54.7(0.999)	42.9(0.992)	29.97
Tricholorethylene	49.2(0.998)	47.3(0.997)	50.7(0.999)	48.5(0.999)	34.62
Tetrachloroethylene	50.7(0.999)	53.8(0.996)	56.9(0.999)	49.7(0.999)	34.68
Benzene	50.4(0.997)	42.3(0.999)	52.7(0.966)	74.8(0.999)	33.92

Regression coefficients (R^2) are given in parentheses.

heat of condensation of the compounds onto the surface, but also from physico-chemical interactions between probes and adsorbents.

5. Conclusion

Catalysts containing 0–2.0 wt% rhodium were prepared and characterized. Inverse gas chromatography was used to characterize the surface properties of H-β-zeolite and Rh/H-β-zeolite. Properties such as enthalpy of adsorption, free energy of adsorption and dispersive and specific components of surface free energy were reported.

The adsorption characteristics of H-β-zeolite can be modified by rhodium. The surface area, the enthalpy of adsorption and dispersive component of the surface free energy decrease after the impregnation of rhodium.

Rhodium has significant effect on the adsorption of benzene. This unique property may be useful for making catalysts for certain reactions involving benzene in the future.

References

[1] X.H. Cui, K. Burgess, Chem. Rev. 105 (2005) 3272–3296.
[2] C.M. Thomas, G. Suss-Fink, Coord. Chem. Rev. 243 (1/2) (2003) 125–142.
[3] A.M. Carroll, T.P. O'Sullivan, P.J. Guiry, Adv. Synth. Catal. 347 (5) (2005) 609–631.
[4] V. Matolin, K. Masek, M.H. Elyakhloufi, E. Gillet, J. Catal. 143 (2) (1993) 492–498.
[5] C.P. Hwang, C.T. Yeh, Q.M. Zhu, Catal. Today 51 (1) (1999) 93–101.
[6] T. Nakatsuji, V. Komppa, Catal. Today 75 (1–4) (2002) 407–412.
[7] R.W. Stevens, S.S.C. Chuang, J. Phys. Chem. B 108 (2) (2004) 696–703.
[8] U.L. Portugal, A.C.S.F. Santos, S. Damyanova, C.M.P.J. Marques, J.M.C. Bueno, J. Mol. Catal. A: Chem. 184 (1/2) (2002) 311–322.
[9] L.P. Qian, Y. Cao, B. Yue, Y. Ren, B.L. Chen, H.Y. He, Chinese J. Catal. 26 (6) (2005) 455–457.
[10] S. Kameoka, K. Kita, S. Tanaka, T. Nobukawa, S. Ito, K. Tomoshige, T. Miyadera, K. Kunimori, Catal. Lett. 79 (1–4) (2002) 63–67.
[11] J. Weitkamp, Y. Traa, Catal. Today 49 (1–3) (1999) 193–199.
[12] K. Yoo, E.C. Burckle, P.G. Smirniotis, Catal. Lett. 74 (1/2) (2001) 85–90.
[13] E.C. Moloy, L.P. Davila, J.F. Shackelford, A. Navrotsky, Micropor. Mesopor. Mater. 54 (1/2) (2002) 1–13.
[14] E. Diaz, S. Ordonez, A. Vega, J. Coca, J. Chromatogr. A 1049 (1/2) (2004) 139–146.

[15] O. Pfohl, R. Dohrn, Fluid Phase Equilibr. 217 (2) (2004) 189–199.
[16] V.I. Bondar, B.D. Freeman, Y.P. Yampolskii, Macromolecules 32 (19) (1999) 6163–6171.
[17] Z.Y. Alsaigh, Int. J. Polym. Anal. Ch. 3 (3) (1997) 249–291.
[18] M.P. Elizalde-Gonzalez, R. Ruız-Palma, J. Chromatogr. A 845 (1/2) (1999) 373–379.
[19] A. Boutboul, F. Lenfant, P. Giampaoli, A. Feigenbaum, V. Ducruet, J. Chromatogr. A 969 (1/2) (2002) 9–16.
[20] E. Papirer, E. Brendle, F. Ozil, H. Balard, Carbon 37 (8) (1999) 1265–1274.
[21] M.A. Montes-Moran, J.I. Paredes, A. Martinez-Alonso, J.M.D. Tascon, Macromolecules 35 (13) (2002) 5085–5096.
[22] A. Askin, D.T. Yazici, Chromatographia 61 (11/12) (2005) 625–631.
[23] F. Tumsek, O. Inel, Chem. Eng. J. 94 (1) (2003) 57–66.
[24] J.H. Xie, Q.L. Zhang, K.T. Chuang, J. Catal. 191 (1) (2000) 86–92.
[25] E. Diaz, S. Ordonez, A. Vega, J. Coca, Appl. Catal. B: Environ. 56 (4) (2005) 313–322.
[26] E. Diaz, S. Ordonez, A. Vega, J. Coca, J. Chromatogr. A 1049 (1/2) (2004) 161–169.
[27] E. Diaz, S. Ordonez, A. Vega, J. Coca, Micropor. Mesopor. Mater. 83 (1–3) (2005) 292–300.
[28] E. Diaz, S. Ordonez, A. Vega, J. Coca, Micropor. Mesopor. Mater. 70 (1–3) (2004) 109–118.
[29] E. Diaz, S. Ordonez, A. Vega, J. Coca, Micropor. Mesopor. Mater. 77 (2/3) (2005) 245–255.
[30] N.A. Katsanos, D. Gavril, J. Kapolos, G. Karaiskakis, J. Colloid Interf. Sci. 270 (2) (2004) 455–461.
[31] E. Diaz, S. Ordonez, A. Vega, J. Coca, Appl. Catal. A: Gen. 295 (2) (2005) 106–115.
[32] N.A. Katasanos, J. Chromatogr. A 1037 (1/2) (2004) 125–145.
[33] N.A. Katasanos, J. Chromatogr. A 969 (2002) 3–8.
[34] N.A. Katasanos, R. Thede, F.R. Kalantzopoulou, J. Chromatogr. A 795 (1998) 133–184.
[35] N.A. Katasanos, J. Kapolos, D. Gavril, N. Bakaoukas, V. Loukopoulos, A. Koliadima, G. Karaiskakis, J. Chromatogr. A 1127 (1/2) (2006) 221–227.
[36] J.A. Navio, G. Colon, M.I. Litter, G.N. Bianco, J. Mol. Catal. A: Chem. 106 (3) (1996) 267–276.
[37] J.H. De Boer, The Dynamical Character of Adsorption, Oxford University Press, London, 1953.
[38] A. Asten van, N. Veenendaal van, S. Koster, J. Chromatogr. A 888 (1/2) (2000) 175–196.
[39] P. Mukhopadhyay, H.P. Schreiber, Macromolecules 26 (24) (1993) 6391–6396.
[40] R.Y. Qin, H.P. Schreiber, Langmuir 10 (11) (1994) 4153–4156.